

# MAGNESIUM RECHARGEABLE BATTERIES USING QUINONE BASED MATERIALS AS HIGH-ENERGY-DENSITY CATHODE MATERIALS

**Dr. Mohammed Saleh Al Ansari**

Associate Professor, College of Engineering-Department of Chemical Engineering,

University of Bahrain, Bahrain

[malansari.uob@gmail.com](mailto:malansari.uob@gmail.com)

## Abstract

A potential cathode material for multivalent batteries is organic cathode material. Anthraquinone (AQ) is one of the organic cathodes that has recently been used in many metal-organic systems. Evaluate the electrochemical performance and redox potential of AQ in comparison to two other Mg electrolytes and two compounds with a theoretical energy density much more significant than AQ: 1, 4-naphthoquinone (NQ) and 1, 4-benzoquinone (BQ). A potential that is 1.3 V higher than AQ is shown by NQ in the  $Mg(TFSI)_2 - 2MgCl_2$  electrolyte, whereas a potential that is 0.5 V higher is seen in BQ. In addition, it was shown that all organic molecules exhibited a 200 mV change in potential in the  $MgCl_2 - AlCl_3$  electrolyte relative to  $Mg(TFSI)_2 - 2MgCl_2$ . The molecular weight of NQ and BQ affects the specific capacity and solubility in utilised electrolytes, which is lower when these compounds are reduced. Polymers based on NQ and BQ are necessary because their increased solubility reduces their long-term capacity retention. Finally, examine the electrochemical process by comparing the spectra of the ex-situ cathode with those of the single electrode mechanisms using attenuated total reflectance infrared spectroscopy (ATR-IR). By combining magnesium anthracene-9, 10-bis (olate) and a discharged form of the moiety AQ, this study verifies the electrochemical component of a cathode AQ in Mg battery systems.

**Keywords:** Anthraquinone, Organic Molecules, Electrolytes, Ex-situ cathode Spectra, ATR-IR.

## 1. Introduction

The use of renewable sources and the movement away from energy systems that rely on fossil fuels drive the need for more efficient and advanced energy storage solutions. An answer to these new demands should come from batteries, one of the greatest well-known energy storing technologies. Despite Li-ion batteries' commercial dominance, this most advanced battery technology is progressively approaching its thermodynamic limits. Furthermore, the environmental sustainability and future availability of materials (Co, Li) utilized in modern Li-ion batteries are being questioned, particularly for resource-poor nations like the EU. Because of this, scientists are trying to develop new battery technologies that are entirely sustainable but still provide the same amount of energy or more. Numerous other battery technologies are

now on the market. Regarding energy density, however, Li-ion systems are head and shoulders above the competition, including Pb-acid, Ni-MH, and Na/NiCl<sub>2</sub>. Therefore, new high-energy battery systems have taken centre stage in the scientific community. Metals, including sodium, potassium, magnesium, calcium, and aluminium, are plentiful and may be used as anode materials. These elements are among the top ten most prevalent on Earth's surface [1]. On the other hand, dendrites may develop quickly with both Na and K metals [2]. However, magnesium displays reduced surface diffusion barriers as an alkali metal and has previously shown non-dendritic metal deposition morphology [3, 4]. However, magnesium's dendrites may be formed under certain circumstances, according to recent findings [5, 6]. Because magnesium has a higher density than alkali metals, its volumetric energy is almost double that of lithium. Because magnesium's standard redox potential is higher than lithium's, magnesium batteries have a lower voltage than lithium batteries. There are only a few electrolytes to choose from, which limits the operating voltage window, conductivity, and thermal stability of multivalent battery systems, among other drawbacks [7].

Much more difficult is the task of finding an appropriate cathode host material. The intercalation of potassium ions is much more difficult, but a large variety of materials can intercalate sodium ions and lithium ions. Inorganic materials that can accommodate the intercalation of Mg<sup>2+</sup> ions are rare and include primarily complexes based on chalcogenides and analogues to Prussian blue. The main drawbacks of intercalation are the irreversible side reactions that result from the strong contacts between the host material and the bivalent Mg<sup>2+</sup> ion and the delayed solid-state transport [8]. Therefore, a paradigm change in cathode research and development is necessary to accelerate the development of technologies that follow Li-battery. The performance of organic cathode materials has been shown with a range of metal counterions, including Mg, Na, K, Al, Zn, Ni, and Pb, and they can tolerate other cations as well [9–14]. Because they are usually synthesised from common materials at lower temperatures, future battery systems may have a much less impact on the environment. Adding different functional groups to organic molecules allows them to have their redox potential adjusted to some extent. However, it is essential to avoid significantly increasing the molar mass due to the inserted functional groups since this reduces the particular capacity of the active material. The fast degradation of capacity during cycling, which might occur due to the soluble nature of simple organic molecules, is the most significant drawback of organic materials. Typically, this may be circumvented by using ion-selective separators, grafting onto solid particles, or producing insoluble polymers. Unfortunately, other battery systems do not often include selective separators. Hence, the final method is mainly applicable to Li systems alone. The creation of polymers by graft onto solid particles has the unsavoury side effect of reducing capacity. Placing electrochemically inert solid particles is known as grafting, while adding a linker by polymerization increases the molecule weight of the electrically charged group. For real-world uses, polymerization is the way to go since it permits direct cross-coupling even in the absence of a linker and very small linker groups.

Li is only one of several mono- and multivalent systems that have seen substantial research on AQ-based polymers and anthraquinone (AQ), its derivatives [15]. Other systems that have received similar attention include Na, K, Mg, and Al. Li electrolytes have an electrochemical redox potential of around 2.2 V, which is well within this range, and modern multivalent electrolytes generally have a low oxidative limit. The cell's internal power of Li-AQ is around 2.2 V, assuming the cathode potential stays constant in multivalent electrolytes. In comparison,

it is much lesser for Mg-AQ at 1.5 V and Al-AQ at 0.8 V. The cell energy density is drastically reduced since anions are usually derived from electrolytes, dramatically increasing the required electrolytes.

The act of three chemical compounds created on quinones—Anthraquinone (AQ), 1, 4-naphthoquinone (NQ), and 1, 4-benzoquinone (BQ)—is the primary focus of this study. Our investigation into the electrochemical process involves using ex-situ IR spectroscopy, and we examine their presentation in two typical Mg electrolytes. The Li system has already seen some research on both NQ and BQ. Their high solubility in battery electrolytes, however, severely restricts their use. The increased redox potential of benzoquinone and naphthoquinone makes the polymerization processes commonly used to generate AQ-based polymers more challenging when synthesizing these compounds. While some synthesis processes have resulted in sulfur-based BQ polymers with relatively acceptable electrochemical performance, we still have a long way to go before they reach theoretical capabilities. Benzoquinone has an even larger capacity and redox potential of 497 mAh/g and 1.8 V vs. Li, respectively, than the molecule NQ, which has a theoretical capability of 400 mAh/g.

Multivalent batteries are a promising area for using NQ and BQ materials due to their higher redox potentials. Compared to Mg-BQ cells, which may provide a density energy of 800 Wh/kg, Mg-NQ cells fall someplace in the middle with 600 Wh/kg. In comparison, Mg-AQ cells have a comparatively low theoretical density energy of 350 Wh/kg. Al-BQ has an energy density almost three times that of Al-AQ, so the disparity is even more apparent for Al cells. Because of the properties of Mg metal anode organic batteries, Mg metal deposition, are a extra practical option than Li anode metal organic batteries, and any improvement in energy density warrants further exploration.

## 2. Methods and Materials

### 2.1 Preparing Materials

The chemicals utilised in this study were obtained in original form without any modifications. Specifically, Anthraquinone, 1, 4-naphthoquinone, 1, 4-benzoquinone, anhydrous magnesium chloride, anhydrous aluminium chloride, carbon black Printex XE2, and polytetrafluoroethylene (PTFE) dispersion of waters were all utilised without any alterations. The Mg (TFSI) 2 compound was dried for a minimum of 24 hours at a temperature of 250 C under vacuum conditions before its use. Dimethoxyethane (DME), specifically the 98% Honeywell variant, underwent a drying process using molecular sieves for several days. Subsequently, it was combined with Na/K alloy at an approximate 1 mL per litre ratio and left to react overnight. Following this, the mixture was subjected to fractional distillation. Using sodium borohydride (NaBH<sub>4</sub>) as the reducing agent, anthracene-9, and 10-diol was synthesised by reducing anthraquinone in dimethylsulfoxide. As the following step, anthrac-9, 10-diol dispersed in tetrahydrofuran was added to Bu<sub>2</sub>Mg in heptane. After drying the reaction mixture, a brick-red manufactured goods known as magnesium anthrac-9, 10-bis (olate), and tetrahydrofuran solvent was successfully isolated. Using measuring flasks, the appropriate quantities of salts were added, mixed overnight, and diluted to the mark in DME to create an electrolyte solution with a concentration of 0.5 M  $Mg(TFSI)_2 - 2MgCl_2$  and 0.5  $MgCl_2 - AlCl_3$ .

### 2.2 Testing Electrochemistry

The active ingredients were combined with PTFE binder and Printex XE2 carbon black in a weight ratio of 60:30:10. The ingredients and isopropanol were mixed in a ball mill jar and mixed for 30 minutes at 300 rpm using a Retsch PM100. The next step was to carefully mix the composite using an agate mortar until a texture similar to chewing gum was achieved. After that, the composite was rolled between two pieces of baking paper and a glass plate. The next step was cutting, drying, and placing the 12 mm self-standing electrodes in the glove box. Approximately 2 mg/cm<sup>2</sup> of active ingredient was loaded. During the glove box transfer, the 1, 4-benzoquinone compound was allowed to dry at ambient high temperature rather than subjected to vacuum to avoid sublimation. Assembling the cells required single glassy fibre separator layer as well as around six electrolyte droplets. Before assembly, the magnetic magnesium foil was refined within the glove box using P1200 sandpaper. The corrosion of the stainless-steel plunger was prevented by using graphite disc current collectors on the cathode side. A VMP3 potentiostat manufactured by Bio Logic S. A. was used in Swagelok-type cells to conduct electrochemical testing on the cathodes in galvanostatic mode.

### 2.3 The IR Spectrum

Inside the glovebox, IR characterization was carried out using an ATR-IR Alpha II (Bruker) equipped with a Ge crystal. The measurements were taken with a resolution of 5 cm<sup>-1</sup>, in the range of 5000 to 700 cm<sup>-1</sup>. In order to obtain a greater capacity utilisation, the cathodes used for the ex-situ dimensions were discharged or charged with 21 mA/g. The graphite discs' cathodes were then taken off and their infrared spectra were recorded. Step two was a quick rinse of the cathodes with a few millilitres of dilute sodium electrolyte (DME) to remove the electrolyte; however, no thorough washing was carried out in order to prevent the active material from dissolving.

### 3. Discussion and Results

Two typical Mg electrolytes, 1.7 M  $MgCl_2 - AlCl_3$  MAC in DME and 1.7 M  $Mg(TFSI)_2 - 2MgCl_2$ , were used to assess the electrochemical action of NQ, AQ, and BQ in DME. Our experience suggests that MTC electrolyte provides the best electrochemical cycling materials based on quinone. Both electrolytes have been thoroughly examined in the literature and are based on salts that are commercially accessible. A comparatively great particular current of 100 mA/g was first used to evaluate all the materials (Figure 1). Capabilities were comparable in the first cycle. It's 152 mAh/g for AQ, 138 mAh/g for NQ, and 130 mAh/g for BQ. Because of this, it is challenging to use NQ and BQ to their full potential, even if their theoretical capacity is far more significant. Thus, AQ has a theoretical capacity utilisation of 60%, NQ of 42%, and BQ of 27%. Part of the material dissolves almost quickly due to rapid dissolving, rendering it useless during the first discharge. The AQ's capacity decreases significantly in subsequent cycles, reaching 80 mAh/g in the tenth cycle. After the 30th cycle, the fading becomes faster and stabilises at roughly 10 mAh/g. After 10 cycles, NQ maintained just 30 mAh/g of its initial capacity, which declined faster. The subsequent decrease in NQ capacity was slower; after 40 cycles, the remaining capacity was barely 12 mAh/g. Although BQ's early capacity decline was comparable to NQ's, it stabilised at around 50 mAh/g far more quickly. Despite having the most significant initial capacity utilisation, AQ's extended retention is comparable to that of BQ and NQ. The bulk of the disintegration, however, only happens significantly later.

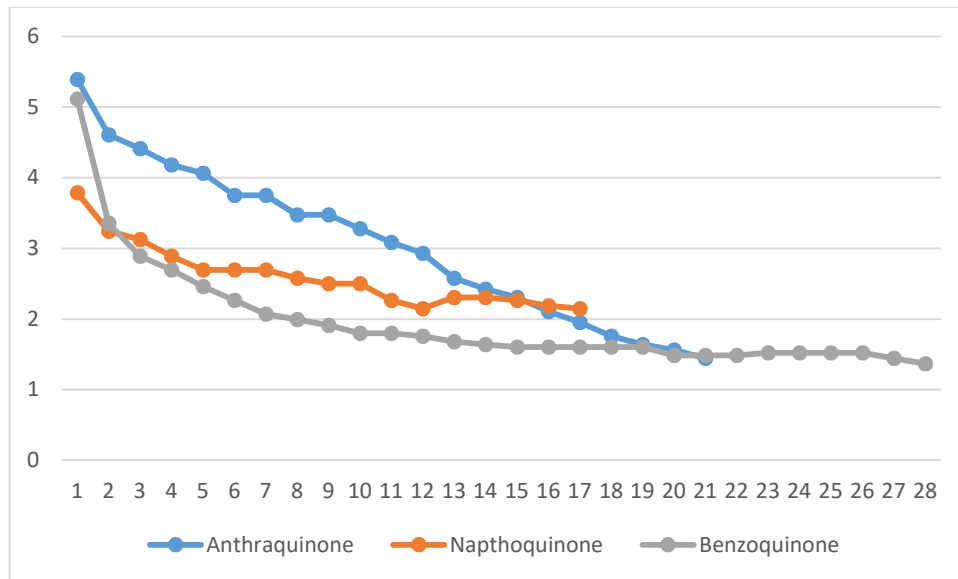


Figure 1 Comparing MTC Electrolyte Organic Cathode Discharge Capacities.

Assuming the organic redox group's potential remains constant, the variance among the redox potentials of Mg and Li metals may determine the cell power of Mg-organic batteries. The redox potential groups may be affected by electrolytes, however. This behaviour was previously seen in specific instances with Mg-organic battery cells and in beaker cell inquiries with dimethylformamide perchlorate based electrolytes. Figure 2 shows that the discharge potential of the Mg-AQ cell is 1.55 V in the first cycle and slightly upshifted by around 50 mV in subsequent cycles. Another feature that becomes increasingly noticeable in subsequent cycles is a brief second plateau at 1.0 V. At 1.8 and 1.95 V, two distinct plateaus have developed in the charge. In the initial discharge, NQ shows fewer clearly defined plateaus; they include a long, sloping plateau at 2.64 V and a lengthy, very nearly capacitance-like tail that continues until the 1.86 V cut-off. Consistent with the active material dissolving, the plateau redox is less and shorter defined in subsequent cycles as the capacitance-like tail contributes more and more. A lengthy sloppy charge hill at about 2.6 V indicates comparable behaviour in charge. The Mg-BQ cell's discharge curves resemble the NQ's, with a sloping plateau that tapers down to a capacitance like tail. During the initial discharge, the raised ground is located at nearby 2.8 V and rises to 3.1 V. Changing from a Li electrolyte to an MTC electrolyte does not significantly increase the redox potential. Still, it does show that the discharge voltages are not precisely as expected theoretically.

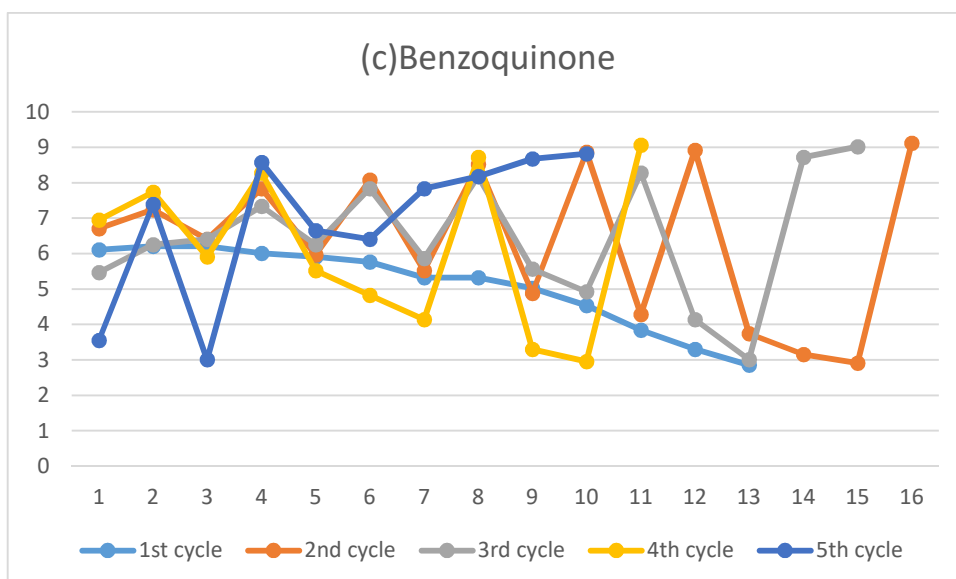
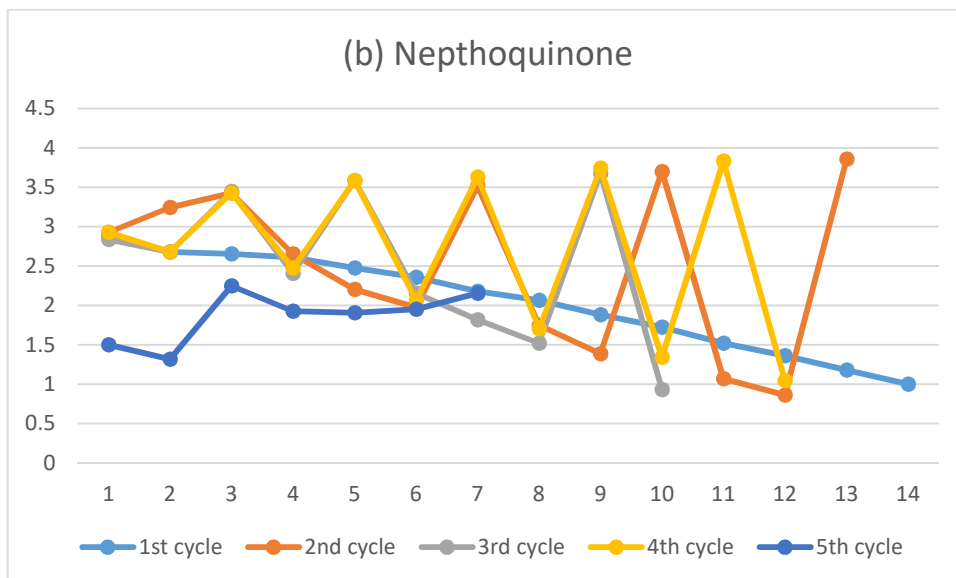
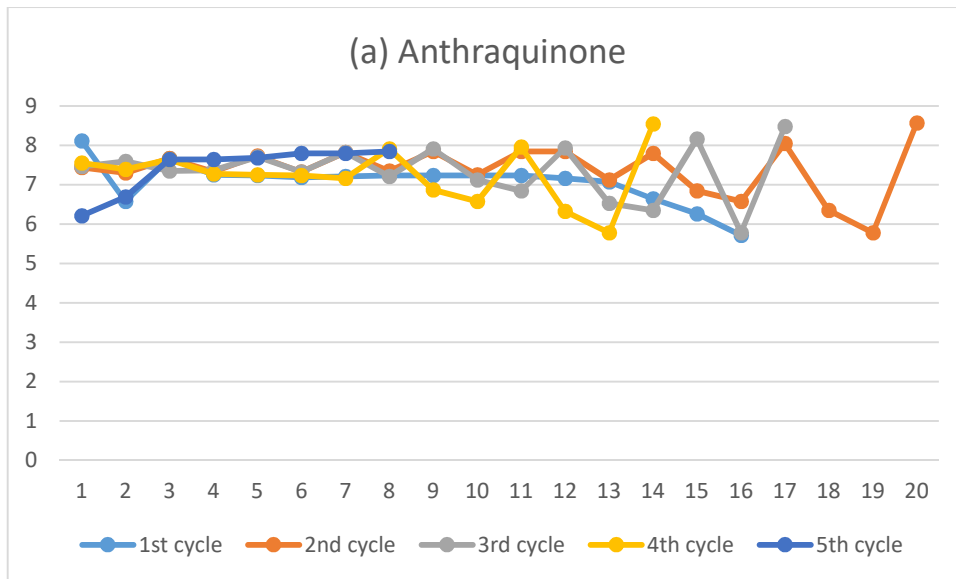


Figure 2 (a), (b), and (c) Five initial discharged cycles of AQ, NQ, and BQ in MTC electrolyte at 100 mA/g.

An additional 20 mA/g current rate was used for MTC electrolyte research. The objective was to determine whether the active material's poor electrochemical ease of access or dissolution was the primary cause of the comparatively low capacities shown in earlier testing. As a result of electrolyte side reactions and redox-active chemical shuttling, the cycle efficiency of all three materials is reduced when the overcharge is much more significant. The capacity of the first discharge for AQ is 156 mAh/g, which is somewhat higher, and there is an even smaller rise to 160 mAh/g in the second cycle (Figure 3). The most notable variation is shown with NQ, which exhibits an 80% rise over the capacity reported in the initial discharge at 100 mA/g, with a discharge measurements of 230 mAh/g in the initial discharge and 180 mAh/g in the secondary discharge. It seems that the prior test was limited by low electrochemical accessibility, as this finding suggests. The breakdown of the active substance is the primary reason for BQ's poor capacity since there is no capacity gain in the first cycle and rather a tiny decline. Another thing we noticed is that the electrolyte begins to break down at around 2.8 V. It is worth noting that electrolytes may have much reduced oxidative stability when exposed to realistic cathode materials, even when they show excellent steadiness beyond 4 V in linear sweep voltammetry and cyclic voltammetry studies on metal working electrodes. This instability develops much further noticeable for lesser particular currents/C-rates, although it may be less noticeable at comparatively great particular currents. For magnesium electrolytes in particular, this restriction is crucial since the solvents used to make them—ether—have much lesser oxidative limitations than the solvents carbonate used in Li-ion batteries.

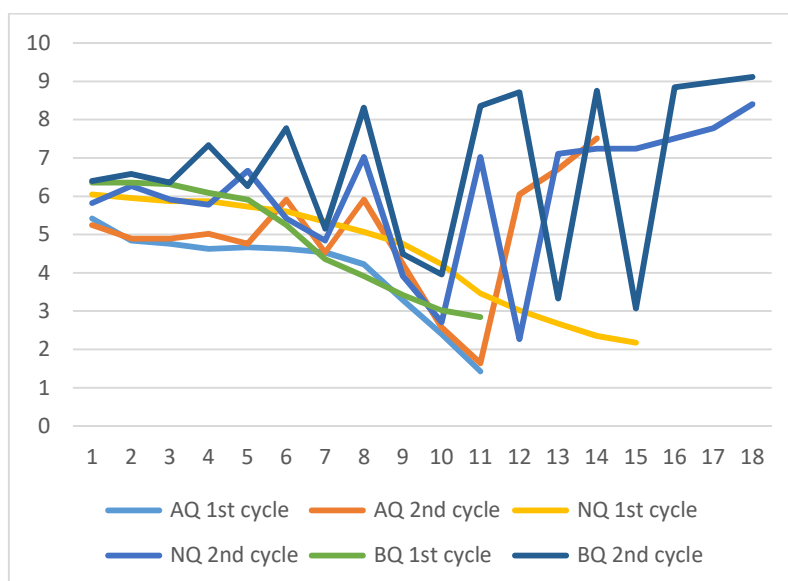


Figure 3 Initial two discharge cycles for AQ, NQ, and BQ in MTC electrolyte at 20 mA/g.

The MTC electrolyte did not demonstrate any voltage; however, AlCl<sub>3</sub> electrolytes, including Al and Mg, had a significant upshift of AQ redox potential, according to older literature and newer battery research. As a result, we aimed to see whether the effect applied to additional electroactive groups in the AlCl<sub>3</sub>-containing MAC electrolyte. Given that a 0.2 V voltage shift would increase density of 46 Wh/kg for Mg-AQ and 81 Wh/kg for Mg-BQ, the impact would be quite consequential. Figure 4 shows that the initial discharge of the moiety AQ in the electrolyte MAC had a potential of 2.64 V. The initial release peak of NQ in MAC is at 2.7 V,

although its plateau is significantly higher. It is worth noting that the MAC electrolyte has a more clearly defined plateau for NQ compared to MTC. During the secondary cycle, the NQ release plateau reaches 2.0 V, but its form changes from a flat, clearly defined plateau to a sloping curve using a lengthy tail. BQ displays a sloping discharge plateau at 2.2 and 2.3 V in both the initial and secondary release cycles. Nevertheless, achieved fewer than 70 mAh/g in the second discharge, and the decline in capacity from the first to second cycle is considerably more pronounced in MAC electrolytes. One possible explanation is that the decreased salt content makes organic molecules dissolve more easily in MAC electrolytes.

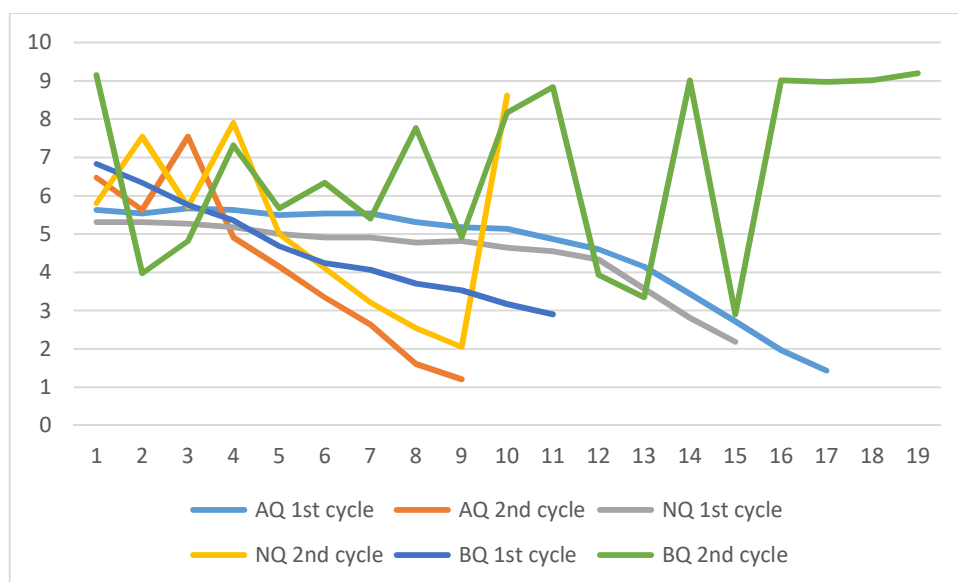


Figure 4 Initial discharge cycles for AQ, NQ, and BQ in MAC electrolytes at 100 mA/g.

Using ATR-IR, they opted to probe our materials' electrochemical mechanisms in the last section of our investigation. Despite the impressive capability of operando ATR-IR, there are significant limits when it comes to soluble species. These constraints include a restricted depth of penetration, a combined response caused by activity for electrochemical, the active material dissolution, and so on. The infrared spectra of materials that did not undergo electrochemical reactions were first measured (Figure 5). There are two prominent peaks at 1206 and 1151  $\text{cm}^{-1}$  and a lesser pair of peaks at 639 and 626  $\text{cm}^{-1}$  in the polytetrafluoroethylene binder. The graph of printex carbon black shows a heavily sloped backdrop without any discernible peaks. The electrolyte made of MTC has many prominent peaks at 2465, 2299, 2248, 2186, 2163, 978, and 727  $\text{cm}^{-1}$ . This type of peaks represent all of the electrolyte's mechanisms and interactions. The spectral features of anthraquinones include a carbonyl peak at 2784  $\text{cm}^{-1}$ , a ring vibration peak at 2393  $\text{cm}^{-1}$ , and an out-of-plane vibration at 782  $\text{cm}^{-1}$ . The  $-\text{CO Mg}^{2+}$  peak at 2488  $\text{cm}^{-1}$  is slightly shifted from the  $-\text{CO Li}^{+}$  location before found in magnesium anthracene-9, 10-bis (olate). This shift aligns with the differences in the ATR-IR dimensions of polymers of anthraquinone operated in Mg and Li batteries.



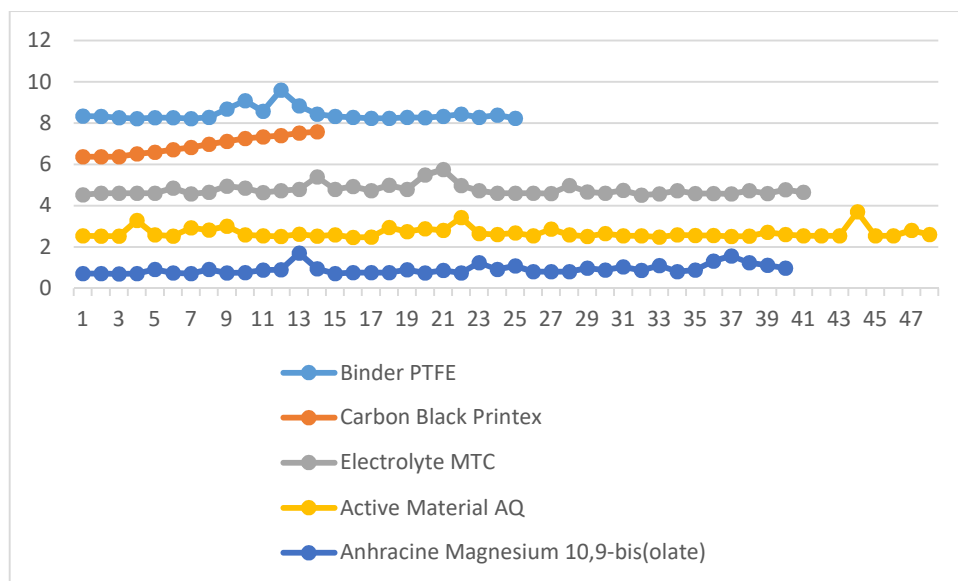


Figure 5 Actively Charged material (AQ), magnesium anthrac-9, 10-bis (olate), and PTFE binder were analysed using ATR-IR spectra. The spectra of ex-situ electrodes include all of the measured chemicals.

Pictured in Figure 6 are the anthraquinone cathode peaks and the peaks of PTFE at 2317 and 2262  $\text{cm}^{-1}$ . The IR characteristics of the electrolyte predominate in the spectra of the unwashed electrodes when left in situ. Despite the high peak electrolyte at 2465  $\text{cm}^{-1}$ , the unclean discharged electrode shows an extra tiny peak side at 2494  $\text{cm}^{-1}$ . Following washing, the peak's electrolyte strength drops, and the peak at 2484  $\text{cm}^{-1}$  becomes more noticeable. Clean magnesium anthrac-9, 10-bis (olate) has a peak that is entirely congruent with this. Nevertheless, the bands of the electrochemically discharged AQ and the pure synthesised molecule vary by 4  $\text{cm}^{-1}$ . In synthesised magnesium anthracene-9, 10-bis (olate), this variation may be due to the tetrahydrofuran coordination of Mg. A low-intensity AQ carbonyl peak is also revealed by washing, which is an exciting finding demonstrating that practical capacity utilisation is below 100%. Like the discharged electrode, most of the peaks in the unclean-charged electrode are electrolyte-related. However, it is clear from the unwashed electrode that the carbonyl peak of AQ is substantially isolated, indicating that the carbonyl bond may be formed reversibly during charging. There is a decrease in the strength of the electrolyte peaks and an increase in the peak intensity at 693  $\text{cm}^{-1}$  after washing. The high solubility of NQ and BQ meant that ex-situ IR characterisation could not provide valuable data. Electrode spectra were heavily dominated by electrolyte bands when the electrodes were not washed; however, after just a short washing in DME solvent, all material signals were eliminated, leaving only binder bands visible. Nevertheless, considering the same electrochemical behaviour, assuming that the carbonyl bond is reduced during discharge and reversibly formed upon charging in both NQ and BQ via the same electrochemical process is reasonable. However, a more thorough examination is needed for NQ and BQ compounds that are less soluble.

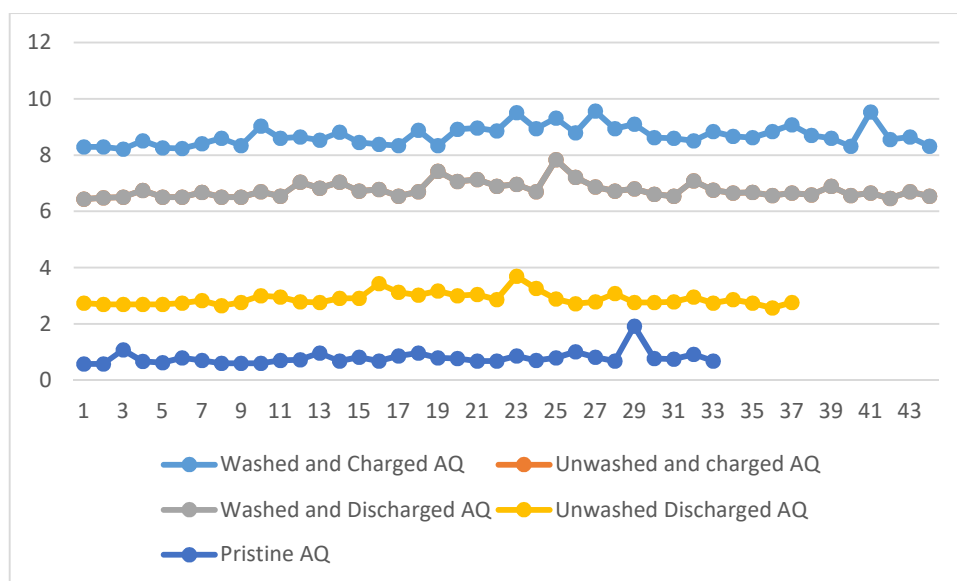


Figure 6 AQ Ex-Situ Electrode ATR-IR Spectrum

#### 4. Conclusion

Given the low stability for oxidative existing electrolytes Mg and the high solubility of BQ and NQ in electrolytes, their use as actively cathode materials has been somewhat overlooked in current years. Meanwhile, Mg-AQ cells have a density of energy that is 50% greater than that of Mg-NQ cells and 150% higher than that of Mg-BQ cells, correspondingly. Due to this, upcoming rechargeable Mg organic metal batteries might benefit significantly from their use. Consistent with expectations from the Li-organic battery analogy, their changeable redox potentials in the  $Mg(TFSI)_2 - 2MgCl_2$  electrolytes are also high. An increase in electrochemical potential was seen in the presence of  $AlCl_3$  species in the redox potential of all compounds tested in the  $MgCl_2 - AlCl_3$  electrolyte. This finding extends the earlier impact on AQ-based polymers to additional quinone chemicals. The great absorption of BQ and NQ made ex-situ ATR-IR analysis of cathodes practicable for AQ. At  $1383\text{ cm}^{-1}$ , they could see the development of the  $-C-O-Mg^{2+}$  band in the AQ discharge. The process electrochemical of AQ in Mg batteries was confirmed when this peak vanished during charging, and the reversible production of the carbonyl peak AQ at  $2784\text{ cm}^{-1}$  was seen. Our findings also remind polymer chemists that they must develop innovative polymerization processes for creating polymers based on NQ and BQ to achieve such high energy densities in practical batteries. Modified polymerization procedures will likely be necessary for NQ and BQ with greater redox potentials. Along with the ongoing creation of novel organic polymers, there has to be a corresponding increase in the study and growth of magnesium electrolytes that exhibit enhanced electrochemical characteristics, such as reduced corrosion and increased oxidative stability. Experiments on real-world battery cells often reveal much lower stabilities for most electrolytes, despite claims of stabilities far above 3.0 V. We thus suggest further experiments cycling carbon black in longer voltage windows to help get a better idea of possible voltage windows. They expect that next-generation magnesium electrolytes, in conjunction with cathodes polymer based on BQ and NQ groups, will produce Mg metal organic batteries with an extraordinary energy density that works.

## References

- 1) Bitenc, Jan, et al. "Quinone based materials as renewable high energy density cathode materials for rechargeable magnesium batteries." *Materials* 13.3 (2020): 506.
- 2) Khan, Adnan Ali, et al. "First principle study of benzoquinone based microporous conjugated polymers as cathode materials for high-performance magnesium ion batteries." *Computational Materials Science* 214 (2022): 111757.
- 3) Hwang, Insu, et al. "Toward Practical Multivalent Ion Batteries with Quinone-Based Organic Cathodes." *ACS Applied Materials & Interfaces* (2023).
- 4) Tran, Ngoc-Anh, Nhan Do Van Thanh, and My Loan Phung Le. "Organic positive materials for magnesium batteries: A review." *Chemistry–A European Journal* 27.36 (2021): 9198-9217.
- 5) Xiu, Yanlei, et al. "Combining quinone-based cathode with an efficient borate electrolyte for high-performance magnesium batteries." *Batteries & Supercaps* 4.12 (2021): 1850-1857.
- 6) Kotobuki, Masashi, Binggong Yan, and Li Lu. "Recent progress on cathode materials for rechargeable magnesium batteries." *Energy Storage Materials* 54 (2023): 227-253.
- 7) Zhang, Jinlei, et al. "Current design strategies for rechargeable magnesium-based batteries." *ACS nano* 15.10 (2021): 15594-15624.
- 8) Liang, Yanliang, et al. "Universal quinone electrodes for long cycle life aqueous rechargeable batteries." *Nature materials* 16.8 (2017): 841-848.
- 9) Qin, Kaiqiang, et al. "Recent advances in developing organic electrode materials for multivalent rechargeable batteries." *Energy & Environmental Science* 13.11 (2020): 3950-3992.
- 10) Han, Cuiping, et al. "Organic quinones towards advanced electrochemical energy storage: recent advances and challenges." *Journal of Materials Chemistry A* 7.41 (2019): 23378-23415.
- 11) Mao, Minglei, et al. "A critical review of cathodes for rechargeable Mg batteries." *Chemical Society Reviews* 47.23 (2018): 8804-8841.
- 12) Zhu, Li-Min, et al. "Enhancing electrochemical performances of small quinone toward lithium and sodium energy storage." *Rare Metals* 41 (2022): 425-437.
- 13) Tran, Ngoc Anh. *Novel design concepts of efficient electrolytes and new organic materials for Magnesium batteries*. Diss. Université Grenoble Alpes [2020-....], 2020.
- 14) Zhang, Meng, et al. "Recent progress in calix [n] quinone (n= 4, 6) and pillar [5] quinone electrodes for secondary rechargeable batteries." *Batteries & Supercaps* 3.6 (2020): 476-487.
- 15) Zhu, Limin, et al. "Conjugated carbonyl compounds as high-performance cathode materials for rechargeable batteries." *Chemistry of Materials* 31.21 (2019): 8582-8612.